Automatic Detection of Single Slow Eye Movements and Analysis of their Changes at Sleep Onset

Filippo Cona[1], Fabio Pizza[2], Federica Provini[2] and Elisa Magosso[1]
[1]*Department of Electrical, Electronic and Information Engineering "Guglielmo Marconi", University of Bologna, Via Venezia 52, 47521, Cesena, Italy*
[2]*Department of Biomedical and Neuromotor Sciences, University of Bologna, Bellaria Hospital, Via Altura 3, 40139, Bologna, Italy*

Keywords: Slow Eye Movements, Sleep Onset, Automatic Detection, Template Matching.

Abstract: An algorithm that can automatically identify slow eye movements from the electro-oculogram is presented. The automatic procedure is trained using the visual classification of an expert scorer. The algorithm makes use of both the spectral and morphological signal information to detect single slow eye movements. On the basis of this detection some parameters that characterize the slow eye movements (amplitude, duration, velocity and number) are extracted. A few possible applications of the algorithm are shown by means of a preliminary study: the average patterns of slow eye movements parameters at sleep onset are evaluated for healthy volunteers and for patients affected by obstructive sleep apnea syndrome. Finally, general considerations are drawn regarding the clinical interest of the study.

1 INTRODUCTION

Eye movements – controlled by a wide neural network involving the cerebellum, brain stem and cerebral cortex – may convey important information on the state and activity of the central nervous system. Eye movements vary from wakefulness to sleep and during the different sleep stages. Since 1968, with the recommendation for visual sleep scoring (Rechtschaffen and Kales, 1968), inspection of eye movements in electro-oculogram (EOG) is routinely performed in clinical polysomnography (PSG) to increase the accuracy and reliability of sleep stage categorization.

In this work we focus on slow eye movements (SEMs), which are pendular, predominantly horizontal eye movements (Aserinsky and Kleitman, 1955); (Värri et al., 1996). SEMs are characteristic of drowsy wakefulness and light sleep (stages 1 and 2), and occur at the beginning and end of sleep (Aserinsky and Kleitman, 1955). In recent years, rising attention has been devoted to SEMs. First, SEM activity at sleep onset has been investigated in relation to other physiological and behavioural measures in order to shed light on the mechanisms underlying wake-sleep transition (Santamaria and Chiappa, 1987); (Ogilvie et al., 1988); (De Gennaro et al., 2000). Furthermore, several studies have specifically investigated SEMs with the aim of identifying early predictor of sleep onset to be used in clinical and occupational settings (Torsvall and Akerstedt, 1987); (Torsvall and Akerstedt, 1988); (Marzano et al., 2007).

The growing interest in SEMs has led to development of various algorithms for automated SEMs detection in EOG, based on different techniques and with different aims. However, some of these algorithms do not identify single SEMs (Värri et al., 1995); (Virkkala et al., 2007); others identify single SEMs, but the validation procedure either exhibits moderate performance (48% sensitivity) (Värri et al., 1996), or is not examined in depth (consisting only in the autodetection/visual scoring ratio) (Hiroshige, 1999); (Suzuki et al., 2001), or is absent (Shin et al., 2011). Moreover, so far none of these studies has characterized SEMs in terms of their parameters (such as amplitude or duration) nor has investigated how SEMs parameters evolve across the sleep onset period.

In recent years, we developed an automatic method for off-line detection of SEM activity in EOG. The method is based on the wavelet transform of two unipolar EOG channels; SEM activity is identified on the basis of EOG power redistribution

Cona F., Pizza F., Provini F. and Magosso E..
Automatic Detection of Single Slow Eye Movements and Analysis of their Changes at Sleep Onset.
DOI: 10.5220/0004551304740481
In *Proceedings of the 5th International Joint Conference on Computational Intelligence* (NCTA-2013), pages 474-481
ISBN: 978-989-8565-77-8

towards higher scales (i.e. lower frequencies) of wavelet decomposition (Magosso et al., 2006). The method was validated against visual scoring on both 8 h and 24 h PSG recordings acquired in a laboratory setting (Magosso et al., 2006); (Magosso et al., 2007); (Magosso et al., 2009). The automatic method for detection of SEM activity was proven to perform reliably in detecting sleep onset in obstructive sleep apnea syndrome (OSAS) patients (Fabbri et al., 2009); (Fabbri et al., 2010). In a further study (Pizza et al., 2011), the algorithm was applied to quantify SEMs distribution during the different sleep stages and across the sleep cycle.

Despite the promising applications of this method, it suffers from some drawbacks that may limit its future use. The main weakness is that the method was conceived, developed and trained to detect SEM activity periods – that may consist of an isolated SEM, a few consecutive SEMs or a long burst of consecutive SEMs – identifying the initial and final instants of each period, but without distinguishing the single eye movements within each SEM period. Hence, the method is not suitable to count the number of single SEMs, nor to extract parameters characterizing each single SEM.

The aim of the present work is to present an advanced version of the algorithm that overcomes the previous limitations and a potential application with some preliminary results. In particular, the new version of the algorithm improves the previous one as to the following points: i) it allows the detection of single slow eye movements in the EOG, segmenting each identified SEM activity period into single movements; ii) more importantly, it is able to extract parameters characterizing each detected slow eye movement.

The proposed algorithm, being able to extract and quantify the parameters of SEMs, may have important clinical implications. In particular, determination of SEMs parameters (number, amplitude, duration, velocity) and analysis of their evolution at the wake-sleep transition may be of value to characterize – by means of quantitative and objective measures – the process of falling asleep in normal, healthy sleepers. This may contribute to a better description and comprehension of the complex process of falling asleep. Moreover, the algorithm can be used to investigate abnormalities of SEMs parameters in patients suffering from sleep-related disorders (such as insomnia, OSAS, narcolepsy), in order to identify potential different SEMs signatures related to different pathologies, which may be of clinical significance. In this regard, the algorithm has been used to assess the evolution of SEM parameters (amplitude, duration, velocity, number) at the wake-sleep transition in healthy volunteers and in OSAS patients, and the obtained results are critically discussed.

2 METHOD

The new version of the algorithm consists of two steps. In the first step, the algorithm identifies SEM activity periods in the EOG: the original version of the algorithm (Magosso et al., 2006), based on EOG wavelet decomposition, has been refined in order to improve its performances. In the second step, the algorithm segments each identified SEM period into single SEMs and extracts some fundamental parameters from the detected movements. The algorithm was trained and validated on the basis of visual identification of SEMs performed by a sleep medicine expert on EOG tracings.

2.1 Data Acquisition

12 healthy subjects and 8 OSAS patients participated in the study. All subjects gave their written informed consent for participation in the study which was conducted with the approval of the local Ethics Committee. The study consisted in a 24 hours PSG recording performed in real-life conditions with a portable digital polygraph (Trex by XLTeck). Volunteers and patients came to the laboratory for about 2 hours in the early morning for device setting, then they left the laboratory, performed their normal life activities for 24 hours and slept at home. The next morning returned to the laboratory for device removing. Recordings included three EEG derivations (F3-A2, C3-A2, O1-A2; filters: 0.5-70 Hz), one submentalis EMG (filters: 30-100 Hz), two EOG derivations (E1-A1, E2-A2; filters: 0.1-15 Hz), and one ECG derivation (filters 1-70 Hz). Each recording was scored by an expert for sleep staging, according to the standard visual criteria (Rechtschaffen and Kales, 1968). Stages were evaluated in 30-s epochs and labeled as wakefulness (W) or as one of the five sleep stages (1, 2, 3, 4 NREM, and REM). Signals are sampled at 512 Hz and resampled at 64 Hz before the processing.

2.2 Visual SEM Scoring

An expert scorer recognized the SEMs on the EOG traces, in particular in a time window around the sleep onset (from 15 minutes before stage 1 to 10 minutes after the beginning of stage 2) and the awakening (from 10 minutes before the end of stage

2 to 20 minutes after the first wake epoch), since these are the moments in which the SEMs are more frequent and distinguishable from other superimposed activity.

An eye movement was identified as an SEM by the expert if it met the following criteria: i) single period of an almost sinusoidal excursion (0.1–1 Hz), beginning and ending at near-zero velocity; (ii) amplitude between 20 and 200 μV; (iii) binocular synchrony with opposed-phase deflections in the two channels; (iv) onsets of the right and left eye movement occur within 300 ms of one another; (v) absence of artefacts (such as blinks, EEG/EMG artefacts). All the parts of the examined EOG portions not identified as SEMs, were defined as Non-SEM (NSEM) activity.

2.3 Identification of SEM Epochs

Following visual detection of single SEMs, the inspected EOG traces were split into 0.5 s epochs: one epoch was defined as an SEM epoch according to the visual classification if at least 50% of the epoch was covered by an SEM marked by the expert; otherwise it was classified as an NSEM epoch. On the basis of this classification we trained a classifier that categorizes each 0.5 s epoch of EOG as belonging to SEM or NSEM periods.

To this end, we calculated the discrete wavelet transform of $\Delta EOG(t) = EOG_R(t) - EOG_L(t)$ (eye movements give opposite contributions to the two electrodes) using Daubechies order 4 as wavelet function, and evaluated 8 scales that approximately cover the frequency bands 16-32 Hz, 8-16 Hz, 4-8 Hz, 2-4 Hz, 1-2 Hz, 0.5-1 Hz, 0.25-0.5 Hz and 0.125-0.25 Hz respectively. From the wavelet coefficients we generated another set of 8 time series $\mathbf{pc}(t) = [pc(1,t),\ldots,pc(8,t)]$: in particular we performed the principal component analysis (PCA) of the logarithm to base 10 of the squared wavelet coefficients. The aim of this processing is to extract power measures, to make their distribution "more normal" and then make them uncorrelated through a change in coordinates.

The 8 quantities pc(n,t) (n = 1,…,8) are resampled with a time resolution of 0.5 s and represent the features used in the classifier. Using the classification of the human scorer we have generated the distributions $P_{n,SEM}(pc(n,t))$ and $P_{n,NSEM}(pc(n,t))$ that represent the probability that a given value of pc(n,t) is observed during SEM and NSEM epochs, respectively. As the features are continuous quantities, the range covering the 98% of each feature distribution was uniformly divided into 20 bins. Figure 1 shows the frequency distributions of the features on visually classified SEM and NSEM epochs (in grey and black respectively).

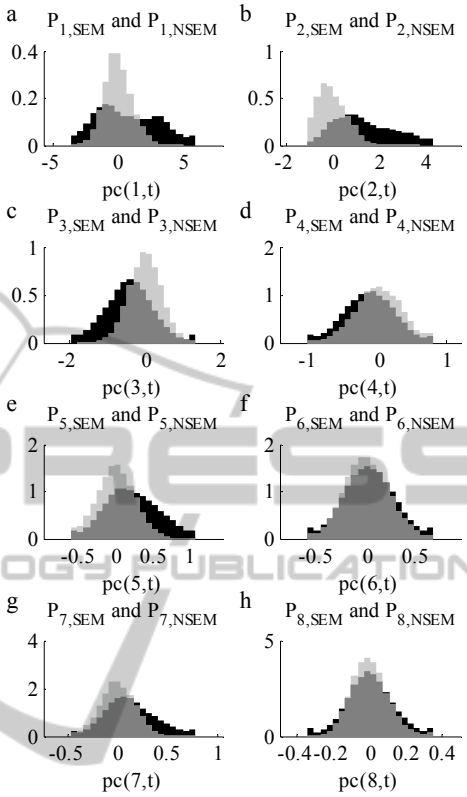

Figure 1: Distributions $P_{n,SEM}(pc(n,t))$ in gray and $P_{n,NSEM}(pc(n,t))$ in black.

The information carried by the 8 values of $\mathbf{pc}(t)$ is then composed into two functions

$$SEM(t) = \prod_{n=1}^{8} P_{n,SEM}\big(pc(n,t)\big) \quad (1)$$

$$NSEM(t) = \prod_{n=1}^{8} P_{n,NSEM}\big(pc(n,t)\big) \quad (2)$$

that represent the likelihood that an EOG epoch at the time t belongs to an SEM or NSEM period respectively. So the EOG epoch at time t is classified as an SEM epoch if SEM(t) > NSEM(t), and as an NSEM epoch otherwise.

The final outcome of this first step is the identification of SEM activity periods in the EOG consisting of a single SEM epoch or consecutive SEM epochs. This first step of the algorithm may be viewed as a refinement of the algorithm previously developed and validated by Magosso and colleagues (Magosso et al., 2006); (Magosso et al., 2007). Indeed, that algorithm was tested only on EOG recorded in clinical settings and showed reduced

performances (results not presented) on EOG acquired in real-life environments.

2.4 Identification of Single SEMs

The next step of the algorithm is devoted to obtain an ideal prototype waveform of SEM, φ(t), to be used as a template to detect single SEMs in each SEM period identified according to the previous step. To generate the SEM prototype all the SEMs identified by the experts have been preprocessed by i) removing biases and slow trends; ii) normalizing them in time (all SEMs have been interpolated to have the same number of time samples) and in amplitude (each SEM has been divided by its standard deviation). In this way, only morphological information is left (figure 2). The generation of this prototype corresponds to training the algorithm for the identification of single SEMs.

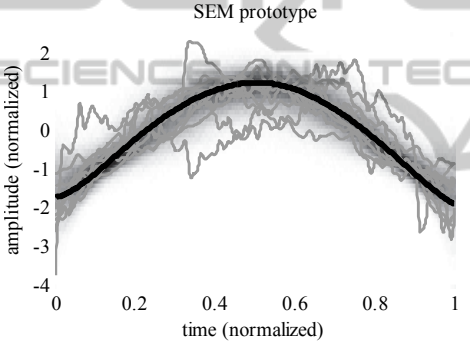

Figure 2: SEM prototype. The grayscale image on the background represents the overall distribution of all the visually scored SEMs (some example are drawn in gray), while the black plot represents their mean, φ(t).

To identify the single SEMs, we implemented an "SEM transform" which is very similar to a continuous wavelet transform, in which the wavelet function is φ(t). The wavelet functions at different scales have been obtained by resampling φ(t): for each length L (in samples) spanning from the shortest to the longest SEM classified by the expert ($L_{min} < L < L_{max}$) we have created a $\varphi_L(k)$, where $k \in \{1, \dots, L\}$ is the resampling index. After the resampling, $\varphi_L(k)$ is treated as if it had the same sampling time as the EOG signal, so the smaller L the smaller the scale of $\varphi_L(k)$.

For each SEM period identified in the first step, we can evaluate the correlation coefficient between the EOG differential mode and each $\varphi_L(k)$, thus obtaining a map of similarity in the time-scale domain. In particular, we computed the correlation coefficient ρ(L,i) between each $\varphi_L(k)$ and ΔEOG(i+k-L/2)

$$\rho(L,i) == \frac{c(L,i)}{\sqrt{\sum_{k=1}^{L} \Delta EOG^2\left(i+k-\frac{L}{2}\right) \cdot \sum_{k=1}^{L} \varphi_L^2(k}} \quad (3)$$

$$c(L,i) = \sum_{k=1}^{L} \Delta EOG\left(i+k-\frac{L}{2}\right) \cdot \varphi_L(k) \quad (4)$$

where c(L,i) represents the correlation. ρ(L,i) has values between -1 and 1, where ±1 indicate perfect match (the concavity of the SEM is not relevant), while 0 indicates complete uncorrelation. A high value of |ρ(L,i)| suggests the presence of an SEM that begins at the time index i-L/2 and ends at time index i+L/2.

Then a path of points (L_n,i_n) is found along this map - where each i_n corresponds to the centre of a SEM of length L_n - that satisfies the following conditions: i) the mean of $\rho(L_n,i_n)$ is maximized; ii) each SEM begins within half second the end of the previous one; iii) the union of all of these SEMs covers completely the SEM period analysed. For the sake of brevity, we will not discuss here the procedure to find the best path that we used in particular, but any optimization algorithm can reasonably work.

At the end of this procedure, each SEM period is subdivided into single SEMs of length L_n and centred in i_n. An example of application is illustrated in figure 3. A 45 s portion of the EOG was recognized by the algorithm as belonging to a SEM period; the SEM period was fragmented into single SEMs on the basis of the similarity with the SEM prototype at different scales and time shifts.

Note that for each of these SEMs, we can easily derive the peak-to-peak amplitude in μV, which is proportional to the correlation $c(L_n,i_n)$, and the duration in seconds, which is proportional to L_n.

2.5 SEMs Parameters Extraction

The present algorithm, being able to identify single SEMs, can extract parameters that characterize the SEM activity. In this work we focused on the amplitude, duration, velocity and the number of the identified SEMs. The algorithm automatically supplies the amplitude and the duration, while the other two parameters can be easily derived.

The n^{th} SEM detected by the algorithm, of length L_n and centred in i_n, can be modelled as

$$\varphi_{fit}(k) = c(L_n, i_n)\varphi_{Ln}(k - i_n) \quad (5)$$

(see for example the panel c of figure 3). It is worth noting that $\varphi_{fit}(k)$ fits the differential EOG.

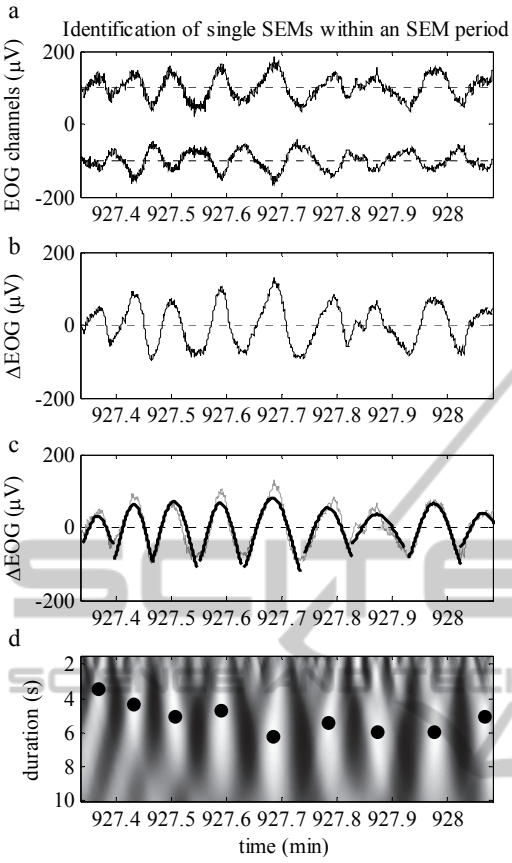

Figure 3: Example of detection of single SEMs in a 45 s EOG trace. Panel a shows the 2 EOG channels; panel b shows the differential mode ΔEOG(t); panel c shows the recognized SEM superimposed to ΔEOG(t); panel d shows the scale frequency map of the correlation coefficient ρ(L,i); the black dots indicate the coordinate (L_n,i_n) of the SEMs detected.

The amplitude (Amp) in μV and duration (Dur) in seconds of the SEM are computed as follows:

$$\mathrm{Amp} = \mathrm{G}\frac{\mathrm{c}(\mathrm{L_n}, \mathrm{i_n})}{2} \tag{6}$$

$$\mathrm{Dur} = \mathrm{L_n} \cdot \Delta\mathrm{t} \tag{7}$$

where G is the ratio between the peak-to-peak amplitude and the standard deviation of φ(t), and Δt is the sampling period of the EOG signal (= 1/64 s). In amplitude computation, the correlation value has been divided by 2, to obtain measures relative to the single EOG channels, rather than their difference (during SEMs the EOG channels have opposite phases, so ΔEOG(t) has double amplitude with respect to the single channels).

The velocity (expressed in μV/s) is taken as the highest mean velocity of the waveform from its beginning, according to the following formulas:

$$\mathrm{v} = \max_{\mathrm{k}} \frac{\varphi_{\mathrm{fit}}(\mathrm{k}) - \varphi_{\mathrm{fit}}\left(\mathrm{i_n} - \frac{\mathrm{L_n}}{2}\right)}{\left[\mathrm{k} - \left(\mathrm{i_n} - \frac{\mathrm{L_n}}{2}\right)\right] \cdot \Delta\mathrm{t}} \tag{8}$$

$$\mathrm{Vel} = \frac{\mathrm{v}}{2} \tag{9}$$

where i_n–$L_n/2$ is the initial time index of the analysed SEM and k is a general time index. As in amplitude computation, the quantity v is divided by 2, to obtain a measure relative to the single EOG channels.

Finally, we consider the number (Num) of SEMs that are recognized in a given time window (e.g. in Sections 3.2 and 3.3 we will consider 5 minutes time windows, so Num will be a measure of frequency of SEMs detected).

A calibration procedure was used to express the values of the SEM amplitude (Amp) in deg and the values of the SEM velocity (Vel) in deg/s.

3 RESULTS

In this section, we briefly present the algorithm performances vs visual scoring. Then we show some results on SEMs parameters evolution in a time window around the sleep onset of the healthy subjects. Finally, the values obtained for healthy subjects are compared with those obtained for OSAS patients. Implications of these differences will be discussed in the Conclusions.

3.1 Validation

A leave one out cross validation has been performed to assess the performances of the algorithm: all the subjects but one were used to estimate the distributions $P_{n,SEM}(pc(n,t))$ and $P_{n,NSEM}(pc(n,t))$ of SEM and NSEM epochs and to construct the SEM prototype; then, the distributions and the prototype φ(t) were used to segment SEMs on the remaining subject. The procedure has been applied 20 times, once for each subject. The performances in the identification of SEM epochs have been assessed in terms of sensitivity (78.1%) and specificity (87.8%). As to identification of single SEMs, only the sensitivity was evaluated (86.0%); the specificity could not be evaluated since the NSEM epochs are not subdivided into single eye movements.

3.2 SEMs Parameters Pattern at Sleep Onset: Healthy Subjects

We analysed the parameters characterizing SEM

activity (extracted as described in 2.5) to describe how they evolve during the transition from wakefulness to sleep in healthy subjects.

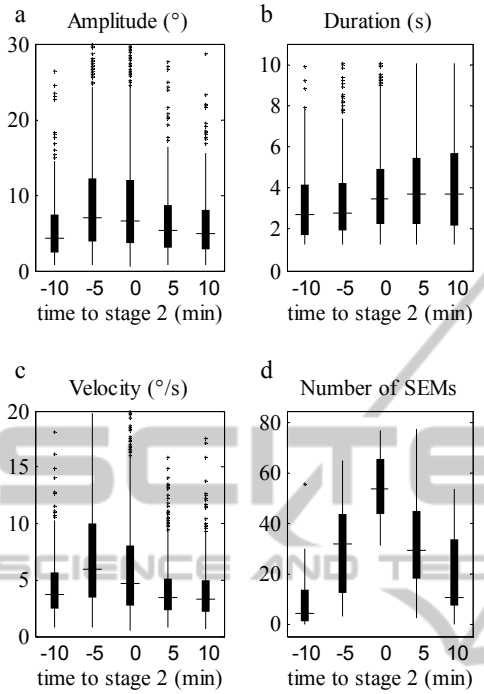

Figure 4: SEM parameters around the sleep onset for the healthy subjects. Panels a, b, c and d show the distributions of the values of Amp, Dur, Vel, and Num in 5 time windows of 5 minutes each.

For each healthy subject, we gathered the values of SEM amplitude (Amp), duration (Dur), velocity (Vel) and number (Num) of the automatically identified SEMs during all the wake-sleep transitions. More specifically, for each transition the time interval from 12.5 min before to 12.5 min after the beginning of stage 2 sleep (first epoch of stage 2 sleep) was considered, and all the wake-sleep transitions occurring in the subjects were aligned to stage 2 onset. The 25 minutes period at the wake-sleep transition was subdivided into 5 bins of 5 min each; all the values of Amp, Dur, Vel and Num of the SEMs occurring in each bin were collected. Then, we have generated 5 distributions for each parameter (one per bin); each distribution is represented by a boxplot (figure 4). Each panel in the figure describes the evolution of the parameter distribution in all the recorded wake-sleep transitions. As shown in figure 4, SEMs amplitude (Amp) has a tendency to grow before the beginning of stage 2, and to decrease afterwards; on the contrary, SEMs duration (Dur) keeps on increasing as sleep deepens. Accordingly, SEMs velocity (Vel) tends to increase before the stage 2 onset, begins to decrease before the beginning of stage 2 and keeps on decreasing afterwards. Finally, as shown by the evolution of Num, SEMs become denser as stage 2 sleep approaches, and gradually become less frequent as sleep further deepens.

To test the significance of these changes we have used a Mann-Whitney U-test to compare the distributions of the parameters between different time bins. In particular, for each parameter, we compared the first bin (-10 min) with the second (-5 min) to assess early changes, the second bin with the third (0 min) to assess changes just before the beginning of stage 2, and the third bin with the last (+10 min) to assess changes that take place as sleep deepens. The amplitude increases significantly several minutes before stage 2 (from -10 to -5 min) and decreases significantly during sleep (from 0 to 10 min). The duration significantly increases later with respect to the amplitude (from -5 to 0 min) while during the sleep it increases by a non-significant amount. Velocity, which is proportional to amplitude and inversely proportional to duration, behaves accordingly: it increases significantly from -10 to -5 minutes and decreases significantly both from -5 to 0 minutes and from 0 to 10 minutes. The number of SEMs also changes significantly on the whole 25 minutes of analysis: it increases before stage 2 and decreases afterwards. The p-values, corrected with Bonferroni correction (24 comparisons, 12 for healthy subjects and 12 for OSAS patients), are given in table 1.

Table 1: p-Values of the statistical analysis for the healthy subjects.

	-10 Vs. -5	-5 Vs. 0	0 Vs. 10
Amp	2.93e-8 ***	5.71	6.32e-10 ***
Dur	9.40	1.58e-7 ***	2.71
Vel	4.14e-9 ***	6.32e-7 ***	4.53e-15 ***
Num	2.20e-3 **	7.20e-3 **	1.01e-4 ***

3.3 SEMs Parameters Pattern at Sleep Onset: OSAS Patients

The same analysis has been performed for the OSAS patients (figure 5). The results suggest that the parameters for this second category of subjects have less significant excursions. Before the sleep, the increase in amplitude is delayed with respect to healthy subjects, becoming significant from -5 to 0 min, rather than from -10 to -5, and the p-values are

globally larger. The duration increases continuously but always by a non-significant amount.

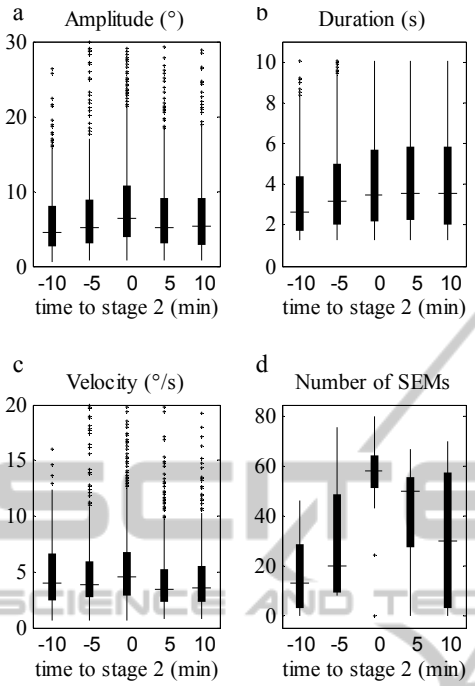

Figure 5: SEM parameters around the sleep onset for the OSAS patients. The panels show the same measures as those of figure 4.

The velocity has a completely different evolution in OSAS patients, since in the second bin it totally lacks the very high values that are observed in healthy subjects. Finally, the number of SEMs follows qualitatively the same evolution as for the healthy subjects, but the changes are not significant. The p-values, corrected with Bonferroni correction (see 3.2), are given in table 2.

Table 2: p-values of the statistical analysis for the OSAS patients.

	-10 Vs. -5	-5 Vs. 0	0 Vs. 10
Amp	6.22e-1	2.49e-4 ***	8.39e-5 ***
Dur	7.99e-2	1.95e-1	16.6
Vel	23.9	2.69e-2 *	1.59e-9 ***
Num	8.85e-1	8.11e-1	6.30e-1

4 CONCLUSIONS

In this work we have presented an algorithm for SEM detection which represents a substantial improvement of our previous version (Magosso et al., 2006; Magosso et al., 2007). Whereas the latter was able to merely detect periods of SEM activity, without segmenting single SEMs, the new algorithm takes advantage of spectral and morphological information to automatically detect single SEMs in EOG, showing high performances vs. visual scoring. Hence, the algorithm is able to count the single SEMs that occurred in a given time window; furthermore, and of great relevancy, the algorithm extracts specific parameters from each recognized SEM, in particular amplitude, velocity and duration.

These new features of the algorithm open important perspectives for basic and clinical research. As SEMs are a phenomenon typical of the sleep onset period, quantification of SEMs parameters and analysis of their evolution at the wake-sleep transition can contribute to improve the understanding of the process of falling asleep. Indeed, this process - although widely investigated - is still far from being fully understood and its comprehension can benefit from a more precise depiction of oculomotor changes. Furthermore, the algorithm may be a valid tool to detect potential modifications of SEMs parameters at sleep onset in patients suffering from sleep-related disorders (insomnia, narcolepsy, OSAS) compared to normal sleepers, thus characterizing abnormalities in the process of falling asleep via quantitative measures provided by SEMs behavior. Regarding to this point, this paper presents some preliminary results obtained on a limited number of subjects. In particular, SEMs parameters in the healthy subjects and OSAS patients seem to exhibit different evolutions at the sleep onset period. On average, in healthy subjects, SEMs parameters change clearly: they increase in number, amplitude and velocity before stage 2 onset; afterwards, SEMs rapidly decrease in number, and change their morphology flattening and lengthening. On the contrary, in OSAS patients, SEMs parameters change by a less amount, exhibiting on the overall a flatter pattern across the five temporal bins that cover the sleep onset period. The obtained results suggest that SEMs might signal differences in the process of falling asleep in the patients compared to normal. The healthy volunteers fall asleep starting from relaxed vigilance state that consists of a few epochs of stage 1 sleep followed by stage 2 sleep and deeper stages later on. On the other hand, the OSAS patients fall asleep with a longer, uneven pattern of vigilance states and they are more prone to wake up from stage 1 and even stage 2 sleep. The absence of a definite evolution of SEMs parameters in OSAS patients could be a marker of the pathological route into sleep. However, it is worth noticing that this

interpretation is far from being conclusive especially because of the reduced size of the OSAS sample; further and deeper analyses with a higher number of subjects are mandatory to confirm these results and eventually disclose other potential explanations.

In future, the algorithm will also be applied to patients suffering from other sleep-related disturbances to provide a depiction of the SEMs signatures in different pathologies.

ACKNOWLEDGEMENTS

This work has been supported by a National project funded by the Italian Ministry for the Environment, Land and Sea *"Excessive daytime drowsiness and road accidents: Specific risks in the transportation of waste and toxic harmful substances of significant ecological impact."*

REFERENCES

Aserinsky, E. and Kleitman, N. (1955). Two types of ocular motility occurring in sleep. *Journal of Applied Physiology*, 8(1), pp.1–10.

Fabbri, M., Pizza, F., Magosso, E., Ursino, M., Contardi, S., Cirignotta, F., Provini, F. and Montagna, P. (2010). Automatic slow eye movement (SEM) detection of sleep onset in patients with obstructive sleep apnea syndrome (OSAS): comparison between multiple sleep latency test (MSLT) and maintenance of wakefulness test (MWT). *Sleep Medicine*, 11(3), pp.253–257.

Fabbri, M., Provini, F., Magosso, E., Zaniboni, A., Bisulli, A., Plazzi, G., Ursino, M. and Montagna, P. (2009). Detection of sleep onset by analysis of slow eye movements: a preliminary study of MSLT recordings. *Sleep Medicine*, 10(6), pp.637–640.

De Gennaro, L., Ferrara, M., Ferlazzo, F. and Bertini, M. (2000). Slow eye movements and EEG power spectra during wake-sleep transition. *Clinical Neurophysiology*, 111(12), pp.2107–2115.

Hiroshige, Y. (1999). Linear automatic detection of eye movements during the transition between wake and sleep. *Psychiatry and Clinical Neurosciences*, 53(2), pp.179–181.

Magosso, E., Provini, F., Montagna, P. and Ursino, M. (2006). A wavelet based method for automatic detection of slow eye movements: a pilot study. *Medical Engineering & Physics*, 28(9), pp.860–875.

Magosso, E., Ursino, M., Zaniboni, A. and Gardella, E. (2009). A wavelet-based energetic approach for the analysis of biomedical signals: Application to the electroencephalogram and electro-oculogram. *Applied Mathematics and Computation*, 207(1), pp.42–62.

Magosso, E., Ursino, M., Zaniboni, A., Provini, F. and Montagna, P. (2007). Visual and computer-based detection of slow eye movements in overnight and 24-h EOG recordings. *Clinical Neurophysiology*, 118(5), pp.1122–1133.

Marzano, C., Fratello, F., Moroni, F., Pellicciari, M., Curcio, G., Ferrara, M., Ferlazzo, F. and De Gennaro, L. (2007). Slow eye movements and subjective estimates of sleepiness predict EEG power changes during sleep deprivation. *Sleep*, 30(5), pp.610–616.

Ogilvie, R.D., McDonagh, D.M., Stone, S.N. and Wilkinson, R.T. (1988). Eye movements and the detection of sleep onset. *Psychophysiology*, 25(1), pp.81–91.

Pizza, F., Fabbri, M., Magosso, E., Ursino, M., Provini, F., Ferri, R. and Montagna, P. (2011). Slow eye movements distribution during nocturnal sleep. *Clinical Neurophysiology*, 122(8), pp.1556–1561.

Rechtschaffen, A. and Kales, A. (1968). *A manual of standardized terminology, techniques and scoring system of sleep stages in human subjects*. Los Angeles, UCLA.

Santamaria, J. and Chiappa, K.H. (1987). The EEG of drowsiness in normal adults. *Journal of Clinical Neurophysiology*, 4(4), pp.327–382.

Shin, D., Sakai, H. and Uchiyama, Y. (2011). Slow eye movement detection can prevent sleep-related accidents effectively in a simulated driving task. *Journal of Sleep Research*, 20(3), pp.416–424.

Suzuki, H., Matsuura, M., Moriguchi, K., Kojima, T., Hiroshige, Y., Matsuda, T. and Noda, Y. (2001). Two auto-detection methods for eye movements during eyes closed. *Psychiatry and Clinical Neurosciences*, 55(3), pp.197–198.

Torsvall, L. and Akerstedt, T. (1988). Extreme sleepiness: quantification of EOG and spectral EEG parameters. *The International Journal of Neuroscience*, 38(3-4), pp.435–441.

Torsvall, L. and Akerstedt, T. (1987). Sleepiness on the job: continuously measured EEG changes in train drivers. *Electroencephalography and Clinical Neurophysiology*, 66(6), pp.502–511.

Värri, A., Hirvonen, K., Häkkinen, V., Hasan, J. and Loula, P. (1996). Nonlinear eye movement detection method for drowsiness studies. *International Journal of Bio-Medical Computing*, 43(3), pp.227–242.

Värri, A., Kemp, B., Rosa, A.C., Nielsen, K.D., Gade, J., Penzel, T., Hasan, J., Hirvonen, K., Häkkinen, V., Kamphuisen, H.A.C. and Mourtazaev, M.S. (1995). Multi-centre comparison of five eye movement detection algorithms. *Journal of Sleep Research*, 4(2), pp.119–130.

Virkkala, J., Hasan, J., Värri, A., Himanen, S. and Härmä, M. (2007). The use of two-channel electro-oculography in automatic detection of unintentional sleep onset. *Journal of Neuroscience Methods*, 163(1), pp.137–144.